Journal of the Korean Physical Society, Vol. 57, No. 6, December 2010, pp. 1624∼1629

Photoluminescence and Lasing Properties of ZnO Nanorods

Geon Joon Lee* and YoungPak Lee
Quantum Photonic Science Research Center, Hanyang University, Seoul 133-791, Korea

Hwan-Hong Lim and Myoungsik Cha
Department of Physics, Pusan National University, Busan 609-735, Korea

Sung Soo Kim and Hyeonsik Cheong
Department of Physics, Sogang University, Seoul 121-742, Korea

Sun-Ki Min and Sung-Hwan Han
Department of Chemistry, Hanyang University, Seoul 133-791, Korea

(Received 8 January 2010)

In this study, we investigated the structures, photoluminescence (PL), and lasing characteristics of the ZnO nanorods prepared by using chemical bath deposition. The continuous-wave HeCd laser-excited PL spectra of the ZnO nanorods exhibited two emission bands, one in the UV region and the other in the visible region. The UV emission band has its peak at 3.25 eV with a bandwidth of 160 meV. However, the PL spectra under 355-nm, 35-ps pulse excitation exhibited a spectrally-narrowed UV emission band with a peak at 3.20 eV and a spectral width of 35 meV. The lasing phenomena were ascribed to the amplified spontaneous emission (ASE) caused by coupling of the microcavity effect of ZnO nanorods and the high-intensity excitation. Above the lasing threshold, the ASE peak intensity exhibited a superlinear dependence on the excitation intensity. For an excitation pulse energy of 3 mJ, the ASE peak intensity was increased by enlarging the length of the ZnO nanorods from 1 μm to 4 μm. In addition, the PL spectrum under 800-nm femtosecond pulse excitation exhibited second harmonic generation, as well as the multiphoton absorption-induced UV emission band. In this research, ZnO nanorods were grown on seed layers by using chemical bath deposition in an aqueous solution of $Zn(NO_3)_2$ and hexamethyltetramine. The seed layers were prepared on conducting glass substrates by dip coating in an aqueous colloidal dispersion containing 50% 70-nm ZnO nanoparticles. Scanning electron microscopy clearly revealed that ZnO nanorods were successfully grown on the seed layers.

PACS numbers: 78.67.Bf, 78.55.-m, 78.30.Fs, 42.55.Zz
Keywords: Lasing, ZnO nanorods, Chemical bath deposition
DOI: 10.3938/jkps.57.1624

I. INTRODUCTION

Photon localization has been of intense interest since it was first proposed as the analogue of electron localization [1]. Nanostructured materials have unique physical and chemical properties as a result of their small size [2]. These properties differ largely from those of the corresponding bulk materials. Experimentally, there have been many research efforts addressing the physical properties of low-dimensional structures, such as nanoparticles, nanowires, nanotubes, quantum dots, and quantum wells [3–9]. Furthermore, semiconductor nanostructures have drawn considerable attention due to their various potential applications, such as light emitting devices, nanolasers, photodetectors, solar cells, biomedical imaging devices and so on [10,11].

ZnO has emerged as a promising optoelectronic material due to its large exciton binding energy of 60 meV and wide bandgap of 3.37 eV [12]. ZnO nanostructures, as well as ZnO films, have gathered considerable attention because of their large nonlinearity, good piezoelectric characteristics, high energy-conversion efficiency, photoluminescence (PL) enhancement, and efficient ultraviolet (UV) lasing [13–17]. ZnO nanostructures can be fabricated by using various methods, such as electro-deposition, chemical bath deposition, chemical vapor deposition, metal-organic chemical vapor deposition, glancing angle deposition, vapor-liquid-solid

*E-mail: glee@hanyang.ac.kr

growth, and molecular scale imprinting [18–20]. Among these fabrication methods, chemical bath deposition is widely used for the fabrication of ZnO nanostructures owing to its simplicity of preparation, satisfactory stability, low-cost equipment, low deposition temperature, and good compatibility with flexible substrates.

In this research, we investigated the structures, PL, and lasing properties of vertically aligned ZnO nanorods. ZnO nanorods were grown on seed layers, by using chemical bath deposition, in an aqueous solution of $Zn(NO_3)_2$ and hexamethyltetramine (HMT). The morphologies and the structures of the ZnO nanorod films were investigated by using scanning-electron microscopy (SEM) and X-ray diffraction (XRD). The optical characterization of the ZnO nanorod films was performed by using UV-visible absorption spectroscopy and linear/nonlinear PL spectroscopy.

II. EXPERIMENTAL DETAILS

Generally, the growth of ZnO nanorods needs nucleation seeds, and their controlled growth requires the spatially-selective modification of the seed layer. According to the literature [21, 22], ZnO films can be used as seed layers for the growth of ZnO nanorods. In this research, the seed layers were prepared on fluorine-doped tin-oxide (FTO) and indium-tin-oxide (ITO) glass substrates by dip coating in an aqueous colloidal dispersion containing 50% 70-nm ZnO nanoparticles (Alfa Aesar, 1314-13-2). The FTO glass substrates were used in most of the experiments, such as the growth of ZnO nanorods, the PL characterization, and the lasing investigation, but the ITO glass substrates were used for absorption spectroscopy of the seed film and the ZnO nanorod films.

The ZnO nanorods were grown on a seed layer, by using chemical bath deposition, in an aqueous solution of $Zn(NO_3)_2$ and HMT [23,24]. Prior to chemical bath deposition, the seed layers were cleaned by using an ultrasonic cleaner for 15 min in soap water, 15 min in distilled water, 15 min in acetone, and 15 min in 2-propanol. The substrate containing the seed layer was placed vertically in a sealed falcon tube containing a 50-$m\ell$ aqueous solution of $Zn(NO_3)_2$ (0.1 - 0.05 M) and HMT (0.1 - 0.05 M). The growth of ZnO nanorods was performed for up to 2 days at 70°C. In order to evaporate the solvent and to remove organic residuals [25], we heat-treated the ZnO-nanorod samples at 300 °C for 1 h.

The morphologies of the ZnO nanorod films were investigated by using SEM (Hitachi, S-4800). The XRD patterns of the ZnO nanorod films were recorded using an X-ray diffractometer (Rigaku, D/MAX-2500) with monochromatized Cu Kα radiation ($\lambda = 1.56$ Å) operated at a voltage of 40 kV and a current of 100 mA. The data were collected in a range of $10° \leq 2\theta \leq 80°$ in the $\theta/2\theta$ mode with a 2θ scanning rate of 0.05°/s. The transmittance spectra of the ZnO nanorod films were measured by using a UV-visible-NIR spectrophotometer (Varian, Cary 500). In order to study the linear PL properties of the ZnO nanorod films, we measured the PL spectra of all the samples at room temperature by using the 325-nm line of a He-Cd laser (Kimmon laser, IK5652R-G) as an excitation light source. In the continuous wave (cw) HeCd laser-excited PL experiment, excitation and collection were normal to the film surface through a microscope objective, and the tight focusing condition was used to increase the excitation beam intensity. The lasing properties of the vertically aligned ZnO nanorods were studied by using high-intensity excitation with a 355 nm picosecond laser pulse from the third harmonic of a mode-locked neodymium-doped yttrium-aluminum-garnet (Nd-YAG) laser. The nonlinear PL spectra were recorded by using a charge-coupled-device (CCD) spectrometer (CVI laser optics, SM-240). The femtosecond PL spectra were obtained by using high-intensity excitation with a 800-nm femtosecond laser pulse from a regeneratively-amplified titanium (Ti): sapphire laser.

III. RESULTS AND DISCUSSION

Figure 1(a) shows a plan-view SEM micrograph of the ZnO nanorod film grown on the seed layer by using chemical bath deposition. The SEM micrograph clearly reveals that ZnO nanorods were succesfully grown on the seed layer by using chemical bath deposition. According to the SEM micrograph and its analysis, the average rod diameter of the ZnO nanorods was about 330 nm, and the density of the ZnO nanorods was $8.4 \times 10^8/\text{cm}^2$. In case of the ZnO nanorods grown for 40 h, the average rod length of the ZnO nanorods was about 1 μm. Figure 1(b) shows the XRD pattern of the ZnO nanorod film. The (002) diffraction peak is located at 33.9°, and its full width at half maximum is as small as 0.98°. This indicates that the crystallization of the ZnO nanorods occurred along the c-axis direction. For the ZnO nanorods prepared by using chemical bath deposition and post theraml annealing, their morphologies, crystallinities, sizes, and shapes can be influenced by various factors, such as the deposition conditions of the seed layer, the process parameters of the chemical bath deposition, and the post-annealing conditions. Figure 1(c) presents the absorption spectrum of the vertically aligned ZnO-nanorod array film. The absorption band edge of the ZnO-nanorod array film is red-shifted with respect to that of the ZnO film. This shift is caused by the optical confinement effect due to the formation of nanorods.

Figure 2 shows the PL spectra of the ZnO nanorod film under cw laser excitation at 325 nm. These PL spectra were measured using four-different excitation intensities. In general, the quantum yield of the PL from an amorphous ZnO film is small. However, the PL intensity can

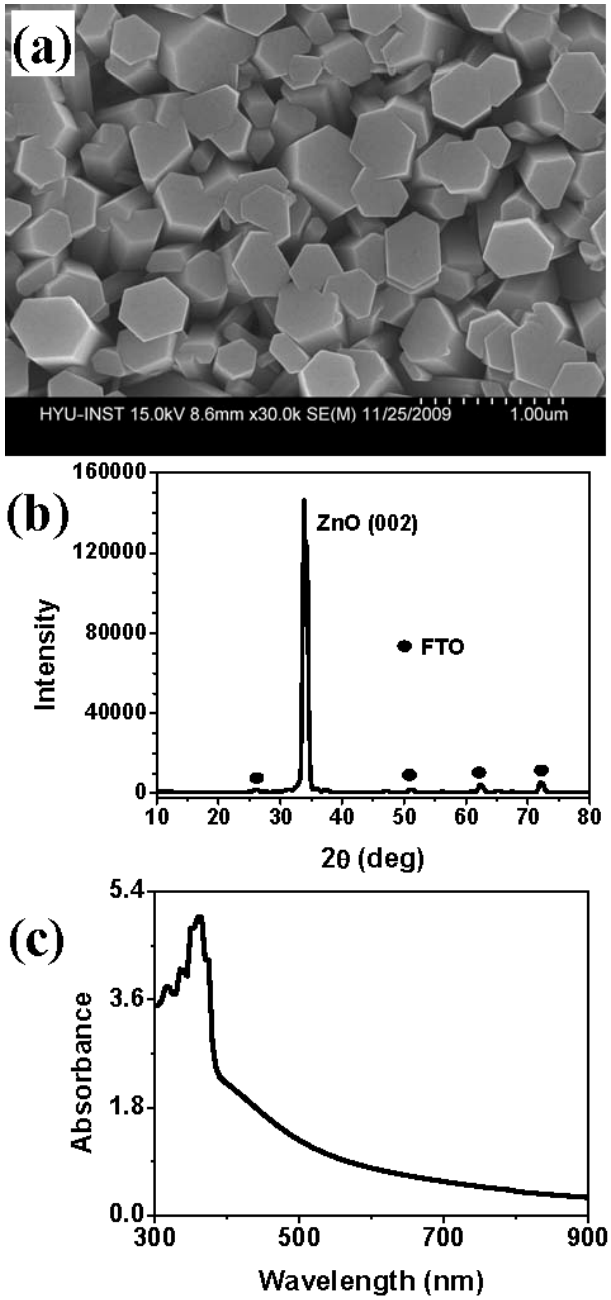

Fig. 1. (a) Typical plan-view SEM micrograph, (b) XRD pattern, and (c) absorption spectrum of the ZnO nanorod film prepared by using chemical bath deposition.

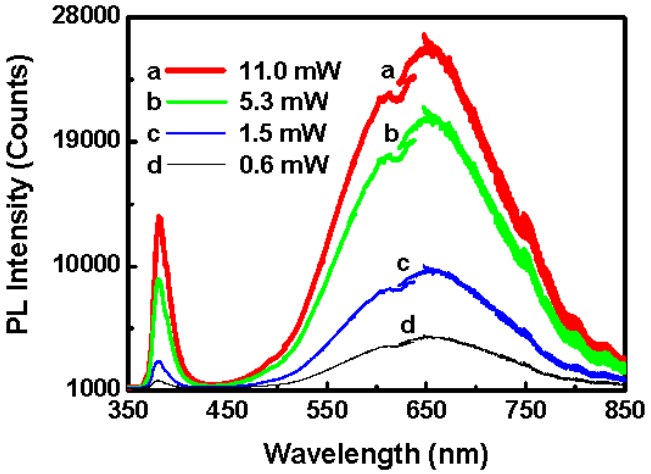

Fig. 2. Continuous-wave HeCd laser-excited PL spectra of the 1-μm ZnO nanorod film for excitation laser powers of (a) 0.6, (b) 1.5, (c) 5.3, and (d) 11 mW. The PL spectra were obtained by using the 325-nm line of a He-Cd laser as an excitation light source.

be enhanced by the formation of low-dimensional structures [13]. Therefore, the formation of crystalline ZnO nanorods results in an enhanced PL as compared with the PL from a ZnO film. Theoretically, the PL spectra of ZnO films or ZnO nanorods consist of two major contributions: One is due to near-band-edge emission that originates from an exciton transition, and the other is the broad visible band due to defect emission that originates from structural defects or impurities [26,27]. As shown in Fig. 2, the cw HeCd laser-excited PL spectra of the ZnO nanorod film exhibited two emission bands, one in the UV region and the other in the visible region. The UV emission band has its peak at 3.25 eV with a full width at half-maximum (FWHM) of 160 meV. The UV band is thought to be ascribed to an efficient exciton emission caused by the formation of a vertically-aligned, closely-packed ZnO nanorod array. Meanwhile, the visible band showed a broad bandwidth of 560 meV. The visible band may related to structural defects. Variation of the ratio of the UV to the visible PL intensities by increasing the excitation laser beam intensity from 0.02 MW/cm^2 to 0.4 MW/cm^2 is small. Here, a beam intensity of 0.4 MW/cm^2 was obtained by tightly focusing a 11-mW laser beam with a 36× microscope objective. These results mean that a beam intensity of $\sim$0.4 MW/cm^2 is insufficient to produce amplified spontaneous emission (ASE) or stimulated emission in our ZnO nanorods. In order to generate ASE or stimulated emission within the lifetime of excitons in ZnO nanorods, an ultrashort pulse laser must be employed as an excitation beam.

Figure 3(a) shows the PL spectra of the 1-μm ZnO nanorod film under excitation by 355-nm picosecond pulses with various excitation pulse energies. These PL spectra were obtained using a picosecond laser pulse with a pulse width of 35 ps, pulse energies from 1 to 3 mJ, and a beam diameter of 8 mm. Under our experimental conditions, a pulse energy of 1 mJ corresponds to a beam intensity of 37 MW/cm^2. In the picosecond laser-excited PL experiment, the excitation and the collection angles were 50° and 0°, respectively. Theoretically, light emission from ZnO nanorods is well known to be the most efficient when the excitation light is polarized along the axial direction of the nanorod [28,29]. Therefore, a p-polarized wave under an oblique incidence geometry al-

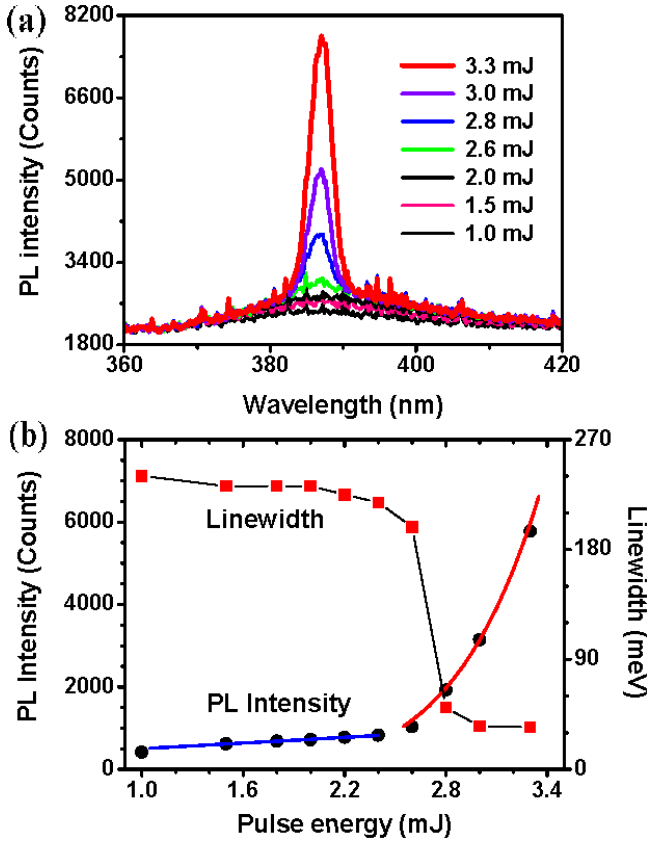

Fig. 3. (Color online) (a) Picosecond pulse-excited PL spectra of 1-μm ZnO nanorod film for various excitation pulse energies. (b) PL peak intensity and PL linewidth as a function of the excitation pulse energy. The PL spectra were obtained by using the 355-nm, 35-ps pulse excitation.

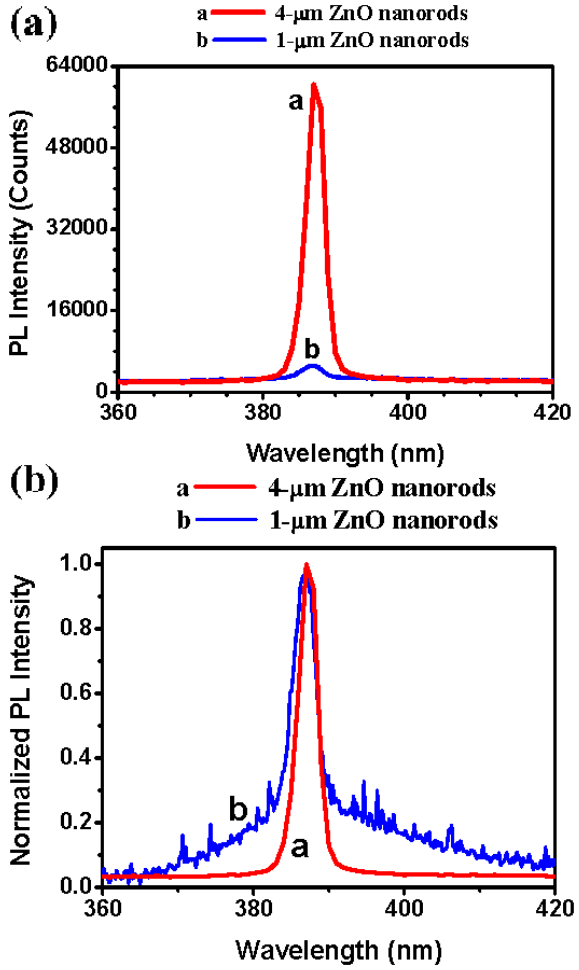

Fig. 4. (Color online) (a) PL spectra of 1-μm and 4-μm ZnO nanorod films under 355-nm picosecond pulse excitation. (b) Normalized PL spectra of 1-μm and 4-μm ZnO nanorod films under 355-nm picosecond pulse excitation. The excitation pulse energy was 3 mJ.

lows more efficient excitation. As shown in Fig. 3(a), ZnO nanorods exhibited a spectrally narrowed emission band with a peak at 3.20 eV and a spectral width of 35 meV. While low-intensity excitation produced a broad UV emission band, high-intensity excitation exhibited a spectrally narrowed UV emission band. The lasing phenomena were ascribed to the ASE caused by coupling of the microcavity effect of ZnO nanorods and the high-intensity excitation.

Figure 3(b) shows the PL peak intensity and the PL linewidth as functions of the excitation pulse energy. The excitation intensity-dependent PL spectra can be summarized as follows: i) As the excitation pulse energy increased beyond the threshold, the PL linewidth decreased from 240 meV to 35 meV. ii) As the excitation pulse energy increased beyond the threshold, the dependence of the PL peak intensity ($I_{PL}^{(peak)}$) on the excitation pulse energy (E_{inc}) changed from a linear intensity dependence ($I_{PL}^{(peak)}$ = a + b*E_{inc}) to a superlinear intensity dependenc ($I_{PL}^{(peak)}$ = a + b*$E_{inc}^{6.8}$). The lasing threshold pulse energy was found to be 2.6 mJ. To summarize, the PL spectra exhibited lasing effects for excitation pulse energies higher than the threshold.

Figure 4(a) shows the picosecond pulse-excited PL spectra of the 1-μm and 4-μm ZnO nanorod films for an excitation pulse energy of 3 mJ. Figure 4(b) presents the normalized PL spectra of the 1-μm and 4-μm ZnO nanorod films. The PL peak intensity of the 4-μm ZnO nanorod film was larger than that of the 1-μm ZnO nanorod film. According to the excitation-pulse energy-dependent PL spectra, the threshold pulse energies of the lasing effects in 1-μm and 4-μm ZnO nanorod films were 2.6 mJ and 1 mJ, respectively. These results are due to the decreased threshold gain (G_{th}) given by the folowing expression [30]:

$$G_{th} = \alpha + \frac{1}{2L} ln \left(\frac{1}{R_1 R_2} \right). \quad (1)$$

Here, L is the length of the nanorod, α is the absorption loss, and R_1 and R_2 are the reflectivities of the end faces.

Figure 5 shows the PL spectrum of the ZnO nanorod

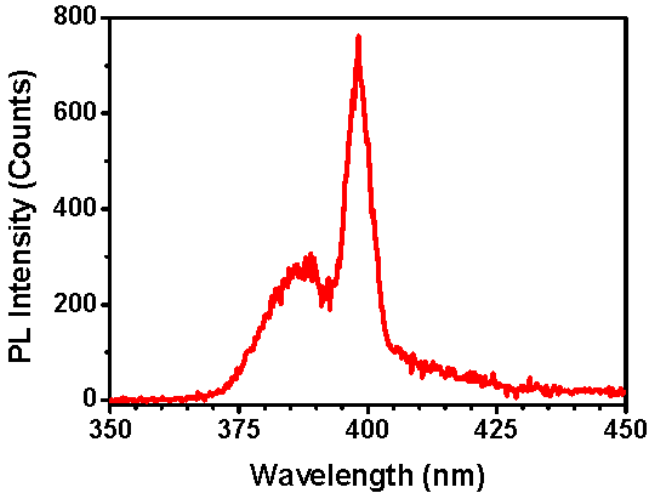

Fig. 5. PL spectrum of 1-μm ZnO nanorod film under 800-nm femtosecond pulse excitation. The excitation pulse energy was 15 μJ.

film under 800-nm femtosecond pulse excitation. The PL spectrum was obtained using a 15-μJ laser beam. The PL spectrum exhibited second harmonic generation, as well as an UV emission band. In this experiment, the exciton emission in the UV region was induced by three photon absorption of the fundamental wave. Meanwhile, the second harmonic wave is thought to be generated from the large optical nonlinearity of the ZnO nanorods.

Precise characterization of the PL properties of the ZnO nanorods, as well as a clear explanation of the lasing mechanism in the ZnO nanorods, have not been satisfied completely so far. In order to further understand the lasing phenomena of ZnO nanorods, it is desirable to perform excitation-power-dependent and excitation-wavelength-dependent PL studies.

IV. CONCLUSIONS

ZnO nanorods were grown on seed layers by using chemical bath deposition in an aqueous solution of $Zn(NO_3)_2$ and hexamethyltetramine. The seed layers were prepared on conducting glass substrates by dip coating in an aqueous colloidal dispersion containing 50% 70-nm ZnO nanoparticles. The SEM micrographs clearly revealed that ZnO nanorods were successfully grown on the seed layers.

The cw HeCd laser-excited PL spectra of the ZnO nanorod film exhibited two emission bands, one in the UV region and the other in the visible region. The UV emission band has its peak at 3.25 eV with a bandwidth of 160 meV. However, the PL spectra under 355-nm, 35-ps pulse excitation exhibited a spectral narrowing phenomena. That is, the picosecond pulse-excited PL spectra exhibited a spectrally-narrowed emission band with a peak at 3.20 eV and a spectral width of 35 meV. The lasing phenomena were ascribed to the ASE caused by coupling of the microcavity effect of ZnO nanorods and the high-intensity excitation. Above the lasing threshold, the ASE peak intensity exhibited a superlinear dependence on the excitation intensity. For an excitation pulse energy of 3 mJ, the ASE intensity was increased by enlarging the length of the ZnO nanorods from 1 μm to 4 μm. In addition, the PL spectrum under 800-nm femtosecond pulse excitation exhibited second harmonic generation, as well as the multiphoton absorption-induced UV emission band.

We expect this research to provide experimental confirmation of the theoretical predictions that ZnO nanorods will exhibit lasing action under high-intensity excitation.

ACKNOWLEDGMENTS

This research was supported by the Basic Science Research Program through the National Research Foundation of Korea grant funded by the Ministry of Education, Science and Technology (Quntum Photonic Science Research Center). Also, this research was supported by the Basic Science Research Program through the National Research Foundation of Korea grant funded by the Ministry of Education, Science and Technology, Korea (Grant number 2010-0009762). M. Cha acknowledges the supports from the Basic Science Research Program through the National Research Foundation funded by the Ministry of Education, Science and Technology (#2008-C00114).

REFERENCES

[1] A. Z. Genack and N. Garcia, Phys. Rev. Lett. **66**, 2064 (1991).
[2] F. Flory and L. Escoubas, Prog. Quantum Electron. **28**, 89 (2004).
[3] Y. Chen, K. Munechika and D. S. Ginger, Nano Lett. **7**, 690 (2007).
[4] L. A. Peyer, A. E. Vinson, A. P. Bartko and R. M. Dickson, Science **291**, 103 (2001).
[5] M. Nirmal and L. Brus, Acc. Chem. Res. **32**, 407 (1999).
[6] G. S. Duesberg, I. Loa, M. Burghard, K. Syassen and S. Roth, Phys. Rev. Lett. **85**, 5436 (2000).
[7] S. Bandow, G. Chen, G. U. Sumanasekera, R. Gupta, M. Gupta, M. Yudasaka, S. Iijima and P. C. Eklund, Phys. Rev. B **66**, 075416 (2002).
[8] S. M. O'Flaherty, S. V. Hold, M. E. Brennan, M. Cadek, A. Drury, J. N. Coleman and W. J. Blau, J. Opt. Soc. Am. B **20**, 49 (2003).
[9] J. P. Richters, T. Voss, L. Wischmeier, I. Rückmann and J. Gutowski, J. Korean Phys. Soc. **53**, 2844 (2008).
[10] V. L. Colvin, M. C. Schlamp and A. P. Alivisato, Nature **370**, 354 (1994).

[11] V. I. Klimov, A. A. Mikhailovsky, S. Xu, A. Malko, J. A. Hollingsworth, C. A. Leatherdale, H. J. Eisler and M. G. Bawendi, Science **290**, 314 (2000).
[12] Ü. Özgür, Y. I. Alivov, C. Liu, A. Teke, M. A. Reshchikov, S. Dogan, V. Avrutin, S. J. Cho and H. Morkoc, J. Appl. Phys. **98**, 041301 (2005).
[13] A. B. Djurišić and Y. H. Leung, Small **2**, 944 (2006).
[14] S. W. Chan, R. Barille, J. M. Nunzi, K. H. Tam, Y. H. Leung, W. K. Chan and A. B. Djurišić, Appl. Phys. B **84**, 351 (2006).
[15] T. Voss, I. Kudyk, L. Wischmeier and J. Gutowski, Phys. Status Solidi B **246**, 311 (2009).
[16] S. Cho, J. Ma, Y. Kim, Y. Sun, G. K. L. Wong and J. B. Ketterson, Appl. Phys. Lett. **75**, 2761 (1999).
[17] G. J. Lee, Y. P. Lee, S. G. Jung, C. K. Hwangbo, S. Kim and I. Park, J. Appl. Phys. **102**, 073528 (2007).
[18] S. M. Lukas and L. M. D. Judith, Mater. Today **10**, 40 (2007).
[19] H. E. Ruda *et al.*, Nanoscale Res. Lett. **1**, 99 (2006).
[20] Z. L. Wang, J. Phys.: Condens. Matter **16**, R829 (2004).
[21] H. Yu, Z. Zhang, M. Han, X. Hao and F. Zhu, J. Am. Chem. Soc. **127**, 2378 (2005).
[22] S. F. Wang, T. Y. Tseng, Y. R. Wang, C. Y. Wang and H. C. Lu, Ceram. Int. **35**, 1255 (2009).
[23] Z. R. Tian, J. A. Voigt, J. Liu, B. Mckenzie, M. J. Mcdermott, M. A. Rodriguez, H. Konishi and H. Xu, Nat. Mater. **2**, 821 (2003).
[24] L. E. Greene, M. Law, D. H. Tan, M. Montano, J. Goldberger, G. Somorjai and P. Yang, Nano Lett. **5**, 1231 (2005).
[25] A. Ennaoui, M. Weber, R. Scheer and H. J. Lewerenz, Sol. Energy Mater. Sol. Cells **54**, 277 (1998).
[26] A. B. Djurišić *et al.*, Nanotechnology **18**, 095702 (2007).
[27] P. T. Hsieh, Y. C. Chen, C. M. Wang, Y. Z. Tsai and C. C. Hu, Appl. Phys. A **84**, 345 (2006).
[28] H. E. Ruda and A. Shik, Phys. Rev. B **72**, 115308 (2005).
[29] H. Y. Chen, Y. C. Yang, H. W. Lin, S. C. Chang and S. Gwo, Opt. Express **16**, 13465 (2008).
[30] B. A. Saleh and M. C. Teich, *Fundamentals of Photonics* (John Wiley & Sons, New York, 1991), Chap. 9.